J. Chem. Sci. Vol. 128, No. 8, August 2016, pp. 1175–1189.
DOI 10.1007/s12039-016-1123-z

On the Attosecond charge migration in Cl·····N, Cl·····O, Br·····N and Br·····O Halogen-bonded clusters: Effect of donor, acceptor, vibration, rotation, and electron correlation

SANKHABRATA CHANDRA, MOHAMMED MUSTHAFA IQBAL and ATANU BHATTACHARYA*

Department of Inorganic and Physical Chemistry, Indian Institute of Science, Bangalore, India
e-mail: atanub@ipc.iisc.ernet.in

MS received 23 January 2016; revised 1 June 2016; accepted 1 June 2016

Abstract. The electron-electron relaxation and correlation-driven charge migration process, which features pure electronic aspect of ultrafast charge migration phenomenon, occurs on a very short timescale in ionized molecules and molecular clusters, prior to the onset of nuclear motion. In this article, we have presented nature of ultrafast pure electronic charge migration dynamics through Cl·····N, Cl·····O, Br·····N, and Br·····O halogen bonds, explored using density functional theory. We have explored the role of donor, acceptor, electron correlation, vibration and rotation in charge migration dynamics through these halogen bonds. For this work, we have selected ClF, Cl_2, ClOH, ClCN, BrF, BrCl, BrOH, and BrCN molecules paired with either NH_3 or H_2O. We have found that the timescale for pure electron-electron relaxation and correlation-driven charge migration through the Cl·····N, Br·····N, Cl·····O, and Br·····O halogen bonds falls in the range of 300–600 attosecond. The primary driving force behind the attosecond charge migration through the Cl·····N, Br·····N, Cl·····O, and Br·····O halogen bonds is the energy difference (ΔE) between two stationary cationic orbitals (LUMO-β and HOMO-β), which together represents the initial hole density immediately following vertical ionization. We have also predicted that the strength of electron correlation has significant effect on the charge migration timescale in Cl·····N, Br·····N, Cl·····O, and Br·····O halogen bonded clusters. Vibration and rotation are also found to exhibit profound effect on attosecond charge migration dynamics through halogen bonds.

Keywords. Attosecond; charge migration; halogen bonds.

1. Introduction

Recently, halogen bonding has been the subject of immense scientific interest for constructing supramolecular assemblies.[1] According to the IUPAC recommendation, "a halogen bond occurs when there is evidence of a net attractive interaction between an electrophilic region associated with a halogen atom in a molecular entity and a nucleophilic region in another, or the same, molecular entity."[2] Therefore, from a simplistic point of view, an intermolecular halogen bond, AX·····B, is formed when two molecules are positioned such that the halogen atom (featured by X) of the electron acceptor molecule (A-X) acts as a bridge to an atom B of another electron donor molecule. In the same configuration, when hydrogen atom takes the place of X in the bridging position, the AH·····B is called the hydrogen bond which is the most conceived noncovalent bond.

In the case of the hydrogen bond, A and B atoms are more electronegative than H atom, and as a result, partially positively charged-H atom is attracted to the lone electron pair(s) of B.[3] In addition, a certain amount of charge is transferred from the B lone pair into a σ^* anti-bonding A-H orbital, which weakens and lengthens the A-H covalent bond. In the case of halogen bond, on the other hand, the bridging halogen atom does not possess a partial positive charge, like the hydrogen bond. Instead, due to highly anisotropic electrostatic potential of the bridging halogen atom, it contains a ring of negative charge that surrounds a crown of positive charge extended along the A-X bond, which is often referred to as a σ-hole.[4] This σ-hole region is attracted to the partial negative charge of the halogen bond acceptor atom B. Similar to the hydrogen bond, there is also a transfer of charge from B atom (usually its lone pair) into σ^* A-X anti-bonding orbital in halogen bond. More discussion on the nature of halogen bonding in comparison with hydrogen bond can be found in recent literature.[1,2,4]

Charge migration through hydrogen bond is an important subject because hydrogen bonds have ubiquitous role in biological electron transport and molecular

*For correspondence

electronics.[5–9] Recently, charge migration through halogen bond has also attracted considerable attention due to its role in novel photosensitive organic materials[10] for the application of organic optoelectronics, solid state lighting, sensing, and imaging. For example, halogen bond helps form complexes such as bromoaromatic aldehyde-based organic crystal[10a] and halopentrafluorobenzene-based liquid crystals.[10c] The former exhibits bright green phosphorescence due to halogen bonding contact, and the latter is used for construction of optically non-linear system. In both the cases, charge migration through halogen bond is proposed to play an important role in their photosensitive functions. In order to harness full potential of the halogen-bonded functional photonic supramolecular materials, however, all aspects of charge migration phenomenon through halogen bonds must be well-understood.

Charge migration is a complex process. This often involves the coupling between nuclear and electronic motions. However, recently, it has been shown theoretically[11–15] that an interesting charge migration can occur in several hundred attosecond timescale, which can be driven purely by the electron-electron correlation and relaxation. This phenomenon can be distinguished from the standard charge transfer model, which is often discussed in the context of Marcus theory and which is driven by the nuclear motion (hence occurs on much slower timescale).[16] The electron-electron correlation-and relaxation-driven charge migration can be initiated immediately following vertical ionization of a molecule or molecular cluster, as demonstrated in recent literature[11–15] and that is why it features pure electronic aspect of charge migration dynamics.

Recently, we have explored pure electron-electron correlation- and relaxation-driven charge migration dynamics through the Cl$\cdots$N halogen bonded clusters following vertical ionization for different A-Cl (A represents F, OH, CN, NH_2, CF_3 and COOH substituents) molecules paired with NH_3 molecule.[14,15] In the vertical ionization scheme, an electron is ejected from the highest occupied molecular orbital (HOMO) and thus, we create a hole in electron cloud of these complexes. Upon removal of an electron from the HOMO of NCCl$\cdots$$NH_3$ complex, the hole is predicted to migrate from the NH_3-end to the ClCN-end of the complex in approximately 500 attosecond. This prediction was made based on both the density functional theory (DFT) and the complete active space self-consistent field (CASSCF) theory. Other halogen bonded complexes, such as H_2NCl:NH_3, F_3CCl:NH_3 and HOOCCl:NH_3 also exhibit similar charge migration following vertical ionization. On the contrary, FCl:NH_3 and HOCl:NH_3 complexes do not exhibit any charge migration following removal of an electron from HOMO, pointing to interesting halogen bond strength-dependent charge migration which is driven purely by electron-electron correlation and relaxation.

In the present work, we have focused on exploring the effects of different donor and acceptors, electron correlation, vibration and rotation on the attosecond charge migration dynamics in halogen bonded isolated clusters. For this investigation, we have selected A-Cl (A represents F, Cl, OH and CN substituents) molecules paired with H_2O (referred as ACl:OH_2 complex) and NH_3 (referred as ACl:NH_3 complex): all these complexes exhibit halogen bonding interactions. We have compared and contrasted the pure electron-electron correlation- and relaxation-driven charge migration dynamics in ionized ACl:OH_2 and ACl:NH_3 complexes.

2. Theoretical Method

In order to explore different facets of pure electron-electron correlation- and relaxation-driven charge migration through halogen bonds, vertical ionization scheme is adopted, which is discussed in detail elsewhere.[14] The process of vertical ionization manifests removal of an electron from a molecular cluster and therefore, it creates a 'hole' in the electronic cloud. The subsequent charge migration dynamics is nothing but the time-evolution of this hole.

As long as we are interested in describing processes that take place before the nuclear dynamics start to play a role, one may consider the frozen frame nuclei at the vertical ion point (vertical ionized geometry corresponds to the neutral optimized geometry) and solve the dynamical Schrödinger equation for the electronic wave function. Recently, it has been shown that the density functional theory (DFT) can be employed for the quantum mechanical treatment of fixed-nuclei-electron dynamics, if correct DFT functional which is free from self-interaction error and which includes long range electron-electron interaction, is used.[17] Therefore, we have used wB97XD DFT functional[18] to explore the hole migration dynamics following vertical ionization of the respective halogen bonded cluster.

The 6-31+G(d,p) basis set is used for all calculations.[14,15] All geometry optimizations and ionization energy calculations are performed using Gaussian 09.[19] Stability of each structure is tested by checking analytical frequencies. The binding energy of the halogen bonded complex is calculated as the difference between the sum of the monomer energies and complex (cluster) energy with correction for basis set superposition error (BSSE).[20]

Vertical ionization of a neutral halogen bonded cluster creates a localized hole. As the electron is removed from highest occupied molecular orbital (HOMO), the initial hole is localized at the HOMO. However, the HOMO of the neutral may not be a stationary orbital of the cation. In that case, the hole charge density may undergo time-evolution. The procedure of quantum dynamics simulation of hole migration dynamics at frozen nuclei of halogen bonded cluster and under one electron approximation is described elsewhere in detail.[14] Briefly, the cationic molecular orbitals are calculated using the unrestricted self-consistent field (unrestricted-SCF) scheme. This scheme renders separate molecular orbitals for α and β spins. The HOMO of the neutral is then projected onto all the stationary cationic molecular orbitals. Thereafter, a time dependent phase factor ($e^{(-iE_\lambda t/\hbar)}$) is introduced to the final equation of the hole orbital. Following this procedure, at time $t = 0$ (immediately after ionization) the hole orbital is mathematically represented as,

$$|\Psi_\alpha(0)\rangle = \sum_{\lambda=1}^{N} \langle \Phi_{\alpha\lambda} | \Psi_{HOMO} \rangle \, |\Phi_{\alpha\lambda}\rangle \qquad (1a)$$

$$\left|\Psi_\beta(0)\right\rangle = \sum_{\lambda=1}^{N} \left\langle \Phi_{\beta\lambda} \middle| \Psi_{HOMO} \right\rangle \left|\Phi_{\beta\lambda}\right\rangle . \qquad (1b)$$

Here, Ψ_{HOMO} represents the canonical HOMO of the neutral, Φ_λ is the λ^{th} cationic molecular orbital of the cluster, $|\Psi_\alpha(0)\rangle$ and $\left|\Psi_\beta(0)\right\rangle$ are the one electron hole orbitals with spin labels α and β, respectively. At a later time (t), the time-evolved hole orbitals are represented as,

$$|\Psi_\alpha(t)\rangle = \sum_{\lambda=1}^{N} \langle \Phi_{\alpha\lambda} | \Psi_{HOMO} \rangle \, e^{(-iE_\lambda^\alpha t/\hbar)} \, |\Phi_{\alpha\lambda}\rangle \qquad (2a)$$

$$\left|\Psi_\beta(t)\right\rangle = \sum_{\lambda=1}^{N} \left\langle \Phi_{\beta\lambda} \middle| \Psi_{HOMO} \right\rangle e^{(-iE_\lambda^\beta t/\hbar)} \left|\Phi_{\beta\lambda}\right\rangle \qquad (2b)$$

3. Results and discussion

3.1 *Structures, Bond Energies and Dynamics*

Previous literature reports show that second order Møller-Plesset perturbation (MP2) theory predicts the interaction energy of halogen bonded clusters with reasonable accuracy.[4,14] Therefore, for the present work, neutral ground state structures of ACl:NH_3, ACl:OH_2, ABr:NH_3 and ABr:OH_2 (where A represents F, Cl, OH and CN substituents) halogen bonded complexes are optimized at the MP2 level of theory with the 6-31+G(d,p) basis set. These structures were also optimized at the wB97XD/6-31+G(d,p) level of theory. Optimized geometries are depicted in Figure 1, along with important structural parameters. For ACl:NH_3, ACl:OH_2, ABr:NH_3 and ABr:OH_2 clusters halogen bond distances are predicted to be in the range of 2.28 to 3.87 Å. Figure 2 illustrates binding energies of ACl:NH_3, ACl:OH_2, ABr:NH_3 and ABr:OH_2 halogen bonded complexes as a function of respective halogen bond distance, computed at the MP2/6-31+G(d,p) and wB97XD/6-31+G(d,p) levels of theory with BSSE correction. Two interesting points are obvious from Figure 2. First, halogen bonding complexes possessing H_2O donor molecule exhibit lower binding energy as compared to similar complexes containing NH_3 donor molecule. This is because H_2O shows less electron donating ability as compared to NH_3 molecule in halogen bonding. Second, halogen bonded complexes comprising Br halogen atom feature higher binding energy than similar complexes containing Cl halogen atom.

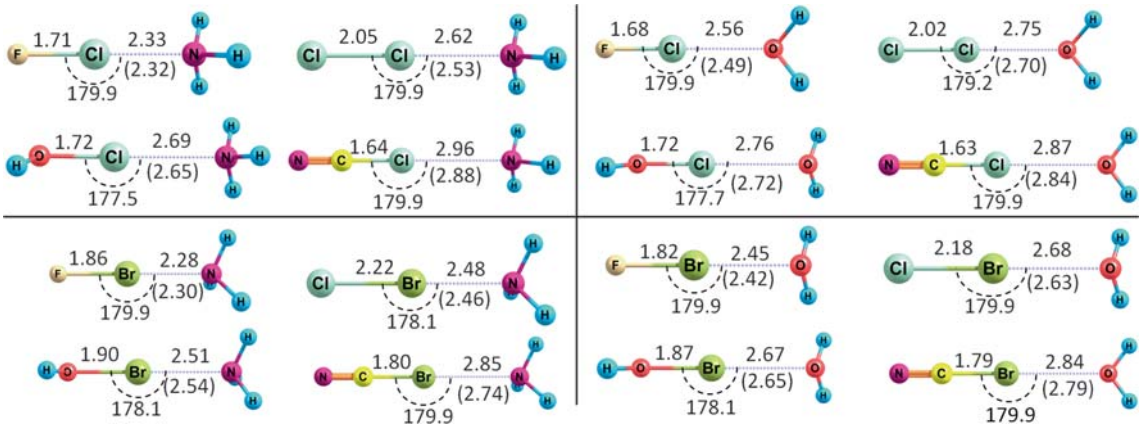

Figure 1. Optimized structures of AX:NH_3 and AX:OH_2 complexes (where, A represents F, Cl, OH and CN substituents and X represents Cl and Br), obtained at the MP2/6-31+G(d,p) and wB97XD/6-31+G(d,p) levels of theory. The wB97XD-results are shown within bracket.

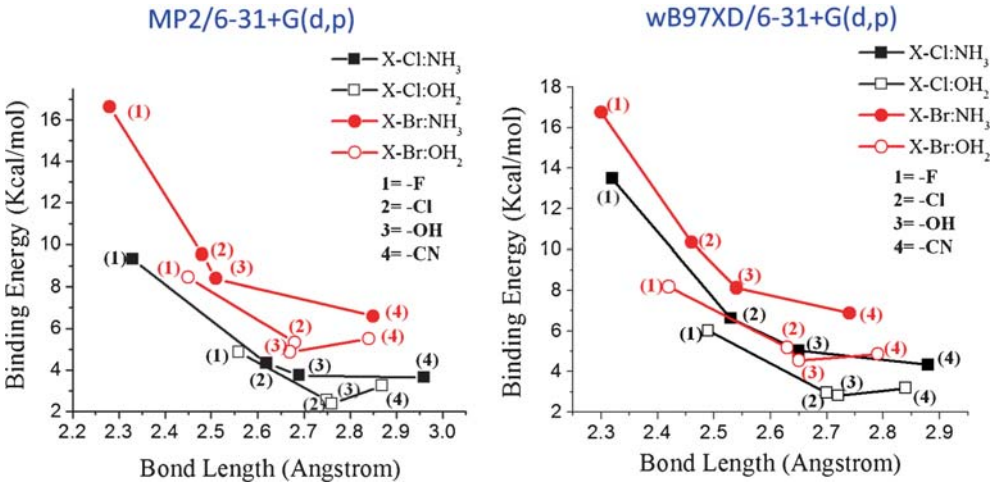

Figure 2. Plot of binding energy plot as a function of X⋯B halogen bond distance, obtained at the MP2/6-31+G(d,p) and wB97XD/6-31+G(d,p) levels of theory.

3.1a *A-Cl:OH*$_2$: In DFT-self consistent field scheme, Kohn-Sham (KS) orbitals can be evaluated as a function of the orbital energy. The highest energy orbital in the restricted-SCF scheme is called the highest occupied molecular orbital (HOMO). Conceivably, a cationic state can be better represented under an unrestricted-SCF scheme because it enables electrons of opposite spin to stay away from one another. Under the unrestricted DFT-SCF-scheme, the KS-orbitals carry a spin level (α or β). Therefore, due to the vertical ionization when an electron is removed from the HOMO, a spatially localized 'hole' is created in the electronic cloud of the HOMO. The HOMO of neutral then represents the hole orbital at the moment of ionization. However, this hole may relax by triggering a time-dependent electron dynamics at the vertical point (at the neutral frozen nuclei configuration). Under the unrestricted DFT-SCF-scheme, lowest unoccupied β molecular orbital (LUMO-β) is the stationary hole orbital of the nascent radical cation under one electron approximation. Therefore, analysis of the neutral HOMO and the cationic LUMO-β at the vertical ion point may predict existence of hole migration in molecular cluster. In order to predict possible hole migration in ACl:OH$_2$

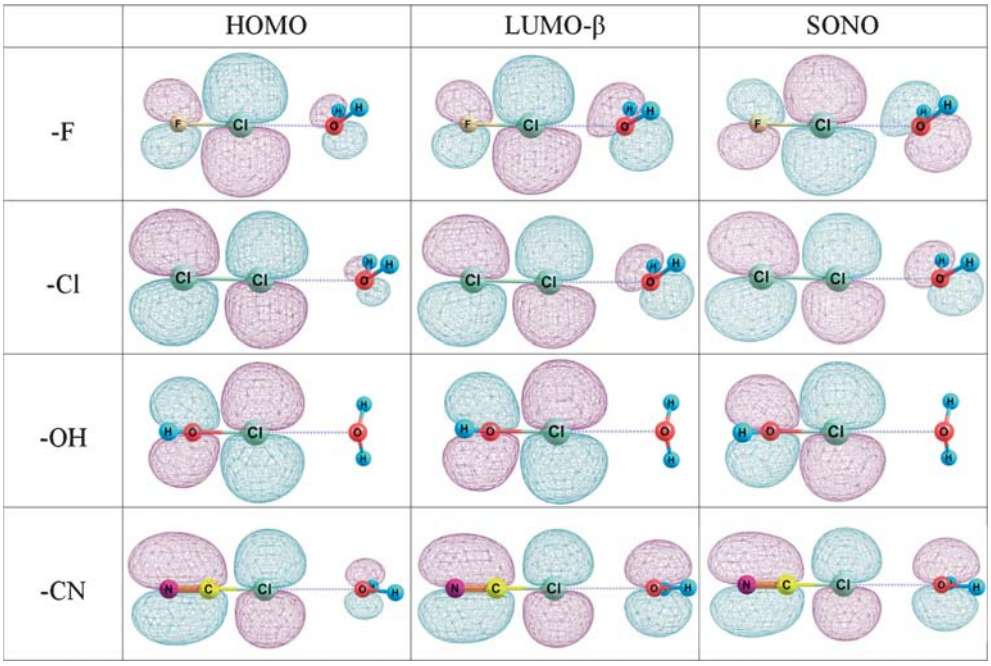

Figure 3. Neutral HOMOs, cationic LUMO-βs and cationic SONOs, calculated at the wB97XD/6-31+G(d,p) level of theory for ACl:OH$_2$ complexes (where A represents F, Cl, OH and CN substituents).

(where, A features F, Cl, OH and CN substituents) complexes, we have first analyzed the neutral HOMO and cationic LUMO β of $ACl{:}OH_2$ complexes at the DFT level of theory.

The canonical HOMO at the neutral singlet surface and the canonical LUMO β at the vertical ion point (VI point, which represents the neutral frozen optimized geometry) on the D_0 surface of $ACl{:}OH_2$ complexes, as computed at wB97XD/6-31+G(d,p), are illustrated in Figure 3. The HOMOs of neutral $ACl{\cdots}OH_2$ complexes clearly exhibit charge (electron) density localized mostly on the ACl-end. Therefore, one can speculate that immediately following vertical ionization, the hole resides on the ACl-end of the respective $ACl{:}OH_2$ complex. Removal of an electron changes the mean field of the electrons, and that is why electrons (in turn, the hole) may undergo relaxation. The cationic LUMO β plots at the VI points on the D_0 surface of $ACl{:}OH_2$ complexes (Figure 3), suggest that the hole density, which was created on the ACl-end, gets delocalized over both H_2O- and ACl-ends in $FCl{:}OH_2$, $ClCl{:}OH_2$ and $NCCl{:}OH_2$ complexes. The hole density in $HOCl{:}OH_2$ complex, however, stays localized purely on the ACl-end of the complex.

We have also analyzed natural orbitals (NO), which are eigenvectors of density operator, for unambiguous assignment of the stationary hole orbital in radical cation at the vertical ion point. Natural orbitals possess occupancy number and the highest occupied natural orbital houses one single electron at the VI point. This is called singly occupied (occupancy number 1) natural orbital (SONO). Figure 3 illustrates that the LUMO βs and the SONOs of cationic $ACl{:}OH_2$ complexes are nearly identical, pointing to the same conclusion that upon removal of an electron by vertical ionization, the hole partially migrates from the ACl-end to the H_2O-end of halogen bonded complexes containing ClF, Cl_2 and ClCN molecules.

The time-propagation of the hole orbital at the VI-geometry of the respective complex is determined using equation 2. Figure 4 shows the hole dynamics in $Cl{\cdots}O$ halogen bonded complexes ($FCl{:}OH_2$, $ClCl{:}OH_2$ and

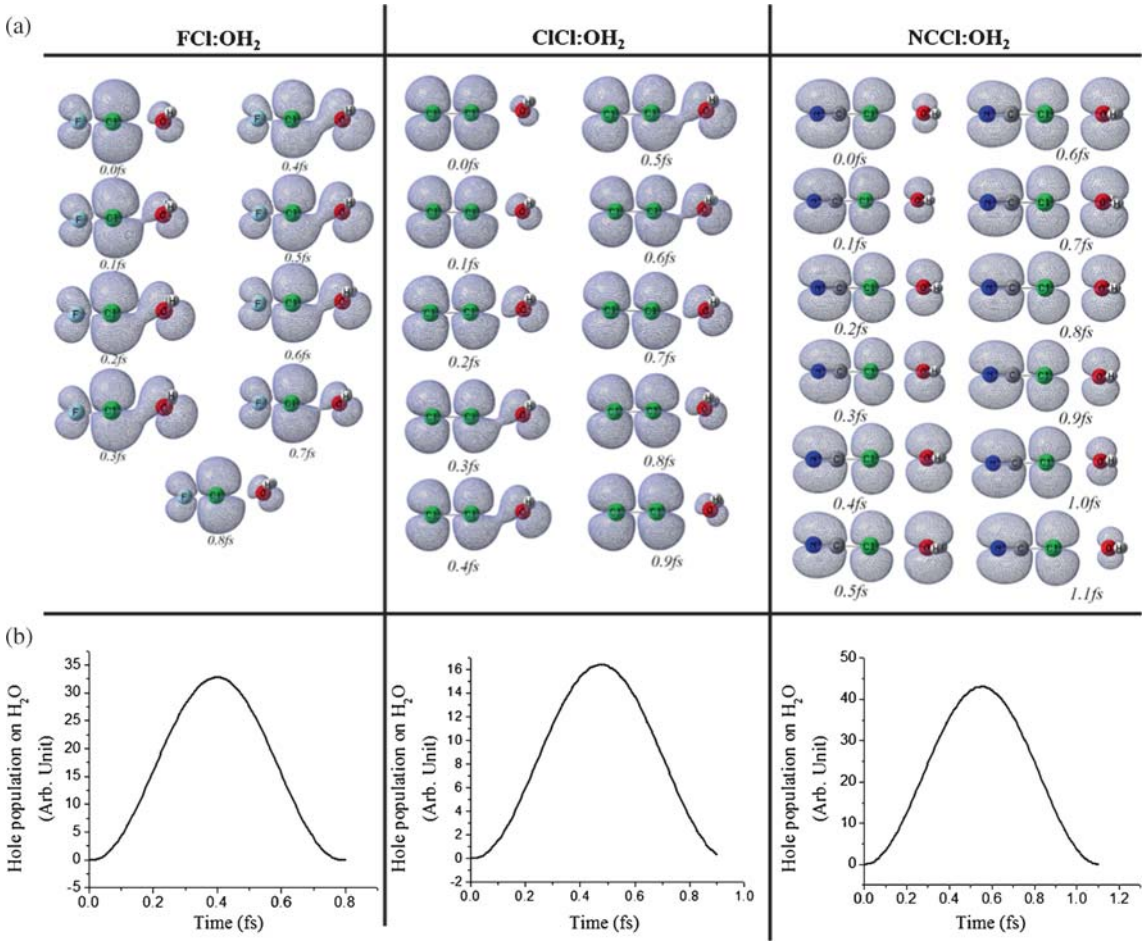

Figure 4. (a) Snapshots of the time-evolution of the hole density following removal of an electron from neutral HOMO of $ACl{:}OH_2$ complexes (where A represents F, Cl and CN substituent) for initial 0–1.1 fs, computed at the wB97XD/6-31+G(d,p) level of theory. (b) Time evolution of the hole population (background subtracted) on the H_2O-end of the respective complex.

$NCCl:OH_2$), obtained at the DFT level of theory with wB97XD functional. Figure 4a shows that the hole orbital at zero attosecond (at the moment of ionization) exhibits hole density mostly localized on the ACl-end of respective $ACl:OH_2$ complexes; however, this hole density rapidly gets delocalized over the Cl·····O halogen bond in approximately 400–600 attosecond. This can be further confirmed from Figure 4b which shows the time evolution of the relative electron population (background subtracted) on the H_2O-end for respective complexes.

3.1b *A-Cl:NH$_3$*: We have presented A-Cl:NH_3 results in our earlier contribution.[14] For reader's perusal, however, we have included A-Cl:NH_3 results in Figure S1 (in Supplementary Information), which depicts the neutral HOMO and the cationic LUMO β for $ACl:NH_3$ (where A features F, Cl, OH and CN) complexes. It is evident in the figure that both the neutral HOMOs and the cationic LUMO-βs are mostly localized on the ACl-end for $FCl:NH_3$, $ClCl:NH_3$ and $HOCl:NH_3$ complexes. On the contrary, the neutral HOMO in $NCCl:NH_3$ complex is found to be mostly localized on the NH_3-end of the complex and respective cationic LUMO-β exhibits a delocalized density over the Cl·····N halogen bond. Therefore, one can conclude that vertical ionization does not initiate charge migration in $FCl:NH_3$, $ClCl:NH_3$ and $HOCl:NH_3$ complexes. $NCCl:NH_3$ complex, on the other hand, exhibits hole migration through the Cl·····N halogen bond following vertical ionization. Time evolution of the hole density in $NCCl:NH_3$ complex is presented in our previous work,[14] which shows charge migration timescale of approximately 500 attosecond from the NH_3-end to the ClCN-end.

3.1c *A-Br:OH$_2$*: Figure 5 depicts neutral HOMOs and cationic LUMO βs for $ABr:OH_2$ complexes. Here A features F, Cl, OH and CN substituents. It is quite evident in the figure that both neutral HOMO and cationic LUMO β densities are identical for $HOBr:OH_2$ complex. This suggests that the hole, which is created by vertical ionization due to removal of an electron from the HOMO, does not migrate in this Br·····O halogen bonded complex. The neutral HOMO densities for other Br·····O halogen bonded complexes, on the other hand, are found to be primarily localized on the ABr-end of the complex and the respective cationic LUMO β densities exhibit that the hole density gets delocalized over the halogen bonded complex. This suggests that the hole partially migrates from the ABr-end to the H_2O-end in $FBr:OH_2$, $ClBr:OH_2$, and $NCBr:OH_2$ complexes following vertical ionization to the D_0 cationic state.

Figure 6 illustrates the hole migration dynamics following vertical ionization (by removal of an electron from the neutral HOMO) of $ABr:OH_2$ complexes (where A represents F, Cl, and CN), computed at the

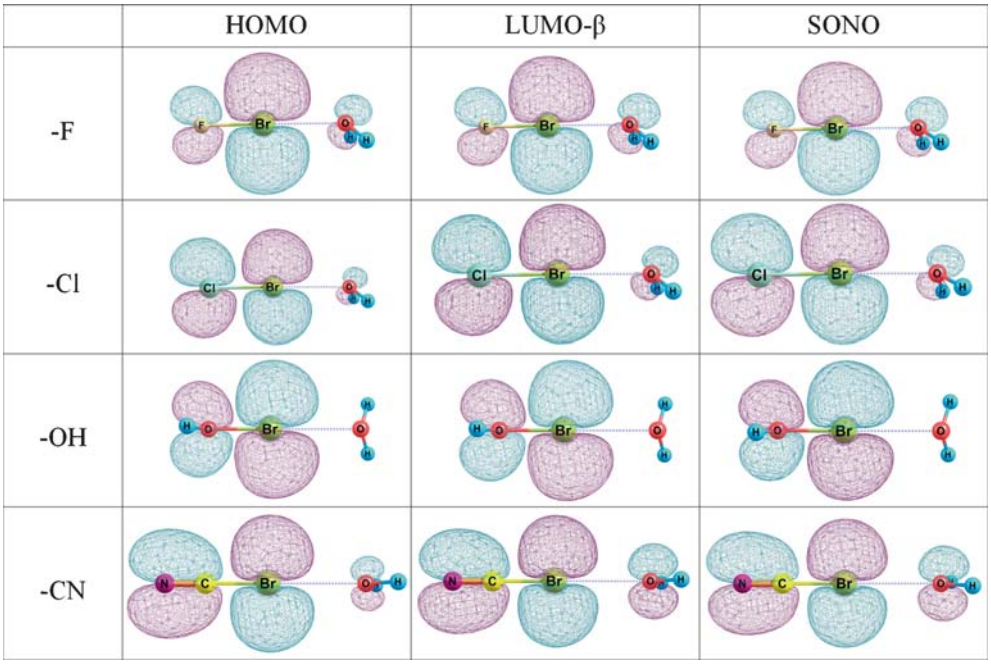

Figure 5. Neutral HOMOs, cationic LUMO-βs and cationic SONOs, calculated at the wB97XD/6-31+G(d,p) level of theory for $ABr:OH_2$ complexes (where A represents F, Cl, OH and CN substituents).

wB97XD/6-31+G(d,p) level of theory. The timescale of charge migration is predicted to be in the range of 300–500 attosecond for these complexes. Furthermore, Figure 6 clearly corroborates the fact that, following removal of an electron from the neutral HOMO of these complexes, the hole partially migrates from the ABr-end to the H_2O-end of the complex.

3.1d *A-Br:NH$_3$*: Neutral HOMOs and cationic LUMO-βs for ABr:NH_3 complexes (A represents F, Cl, OH and CN substituents), as computed at the wB97XD/6-31+G(d,p) level of theory, are depicted in Figure 7. The neutral HOMO densities for all the Br⋯N halogen bonded complexes are found to be purely localized on the ABr-end. Similarly, cationic LUMO βs are also predicted to be localized on the same ABr-site for FBr:NH_3, ClBr:NH_3 and HOBr:NH_3 complexes; whereas, the cationic LUMO β for NCBr:NH_3 complex exhibits density delocalized over the Br⋯N halogen bond. This result indicates that the charge does not migrate in Br⋯N halogen bonded complexes containing BrF, BrCl, and BrOH molecules. However, NCBr:NH_3 complex shows charge delocalization upon vertical ionization. The time-evolution of the respective hole density, which is shown in Figure 8, further corroborate the same fact. Hole delocalization in NCBr:NH_3 complex occurs in approximately 500 attosecond timescale.

3.2 *Comparison*

In general, halogen bonded complexes show a common geometrical notation, expressed by A-X⋯B, pointing to qualitative similarity among these noncovalent bonding interactions. However, the potential of one type of halogen bond over other in photonic crystal engineering arises more from its differences, than from the similarities to each other. Differences may arise from several

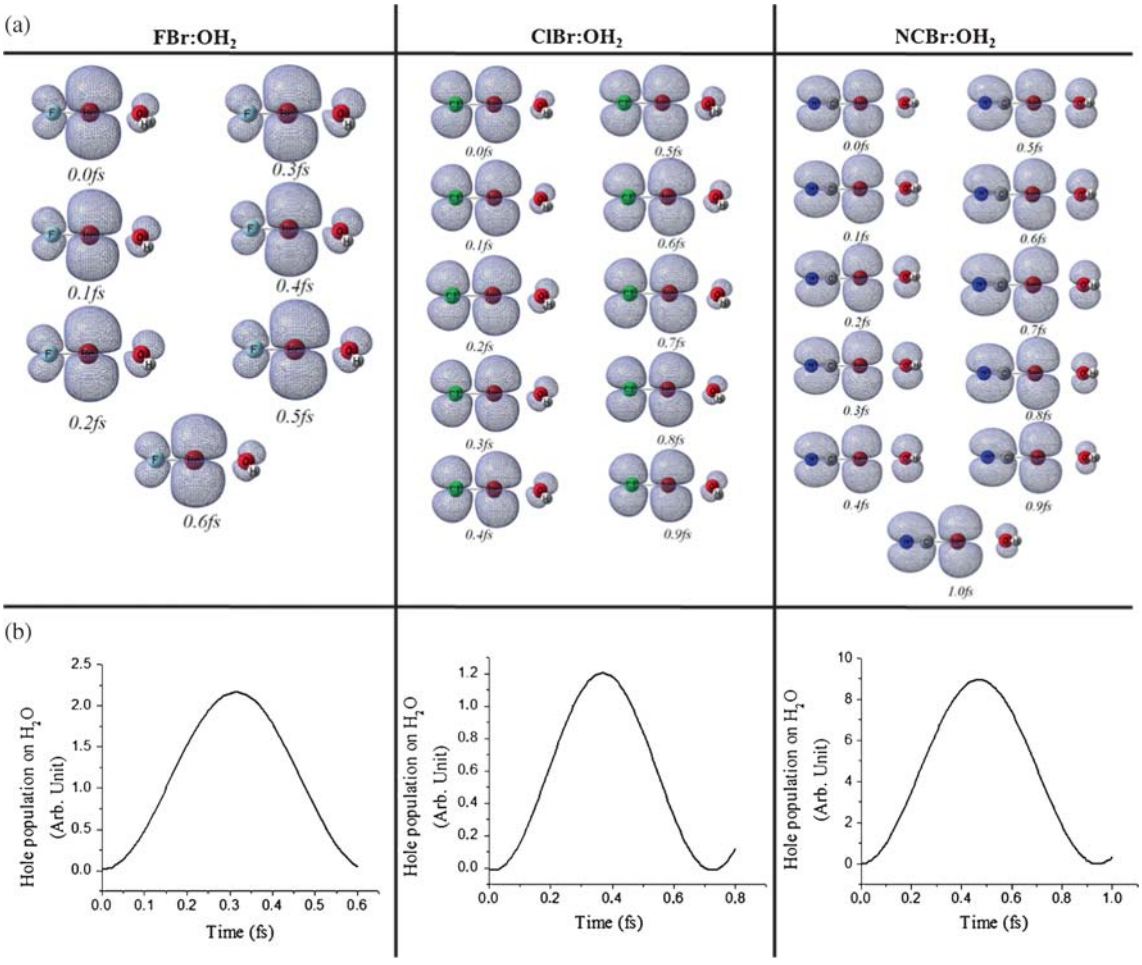

Figure 6. (a) Snapshots of the time-evolution of the hole density following removal of an electron from HOMO of neutral ABr:OH_2 complexes (where A represents F, Cl and CN substituents) for initial 0–1 fs, computed at the wB97XD/6-31+G(d,p) level of theory. (b) Time evolution of the hole population (background subtracted) on the H_2O-end of the respective complex.

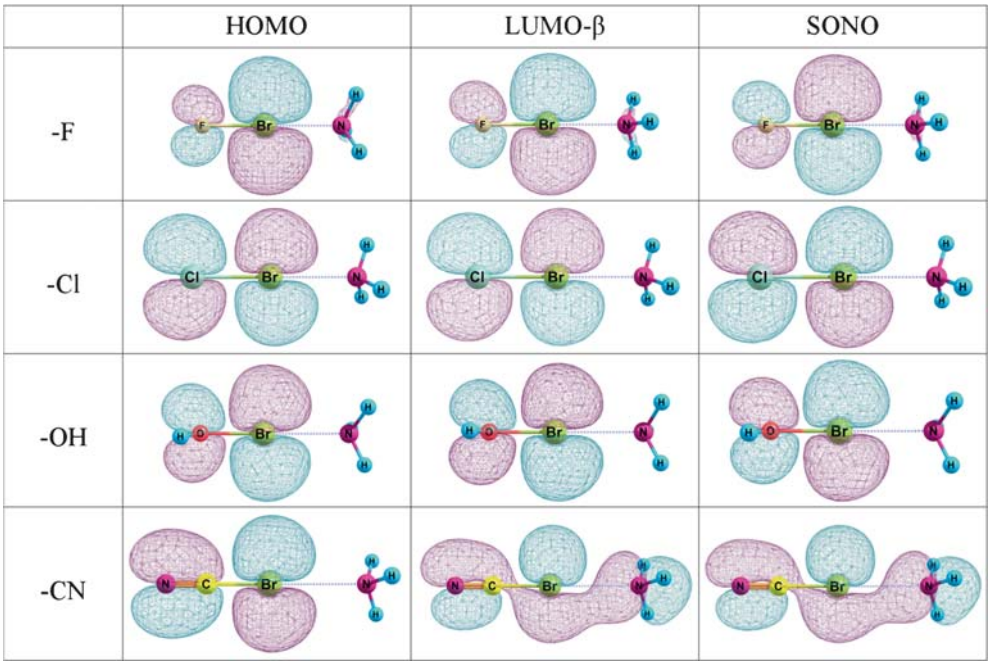

Figure 7. Neutral HOMOs, cationic LUMO-βs and cationic SONOs calculated at the wB97XD/6-31+G(d,p) level of theory for ABr:NH_3 complexes (where A represents F, Cl, OH and CN substituents).

factors, such as directionality, hydrophobicity, donor atom size, and electron withdrawing ability.[1,2,4] In spite of several differences found in bonding nature of different halogen bonds (e.g., Cl····N, Cl····O, Br····N and Br····O), our present work shows that timescale of electron-electron relaxation and correlation-driven charge migration through these bonds falls in the range of 300–600 attosecond. This observation points to existence of a universal response time range for electron-electron correlation and relaxation-driven

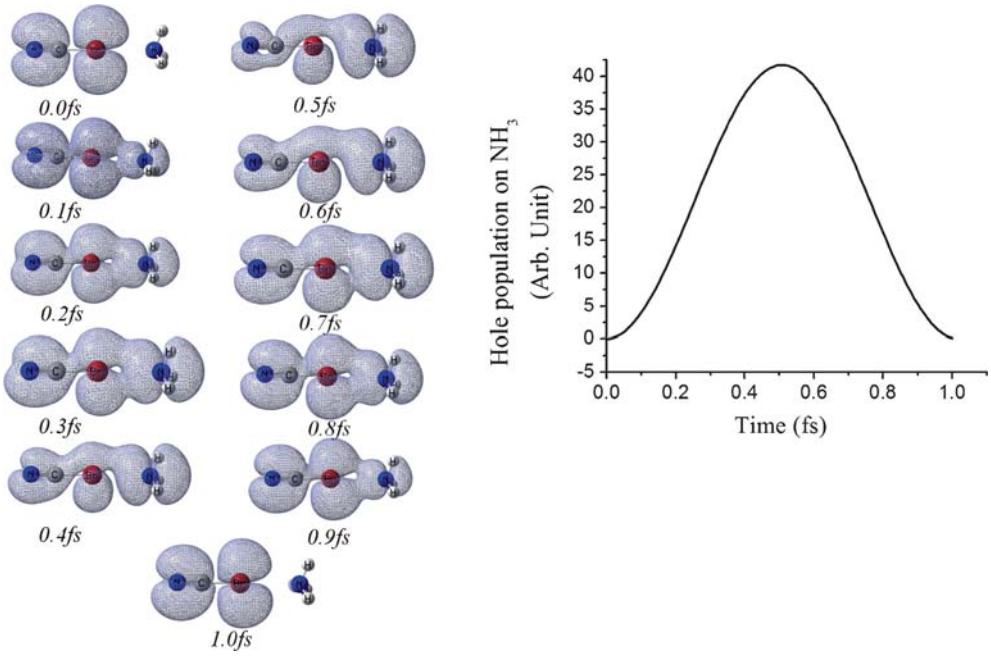

Figure 8. Snapshots (left) of the time-evolution of the hole density following removal of an electron from neutral HOMO of NCBr:NH_3 complex for initial 0–1 fs, computed at the wB97XD/6-31+G(d,p) level of theory. Time evolution of the hole population (background subtracted) on the NH_3-end is also plotted (right).

charge migration dynamics through halogen bonds. However, in the present discussion the first question which comes to our mind is why does charge migration occur in some complexes and why don't some exhibit the same?

3.2a *Driving Force behind Charge Migration*: Vertical ionization of a neutral cluster creates a localized hole in the neutral HOMO. This hole density may evolve in time, since neutral HOMO density may not be one electron stationary state of the cation. The weights of neutral HOMO on all stationary cationic molecular orbitals (represented by $|\langle\Phi_{\alpha\lambda}|\Psi_{HOMO}\rangle|^2$ for α-cationic orbitals and by $\left|\left\langle\Phi_{\beta\lambda}\middle|\Psi_{HOMO}\right\rangle\right|^2$ for β-cationic orbitals, as defined in equation 1, under unrestricted-SCF scheme) are shown in Figure 9, taking examples of NCA:NH_3 and NCA:OH_2. Figure 9 shows that the initial hole density (or in other words the HOMO density) is mostly a linear combination of two stationary cationic MOs, namely LUMO-β and HOMO-β, for NCCl:NH_3, NCCl:OH_2, NCBr:NH_3 and NCBr:OH_2 complexes. These MOs are also depicted in Figure 9. As expected from Figure 9, therefore, the period (τ) for the hole migration is nothing but an oscillation of the charge between these two stationary orbitals. This is why the timescale ($\tau/2$) of the oscillation is defined by the energy difference (ΔE) between these two stationary cationic orbitals ($\tau = h/\Delta E$). For example, ΔE is found to be 3.69, 3.74, 4.07, and 4.39 eV for NCCl:NH_3, NCCl:OH_2, NCBr:NH_3, and NCBr:OH_2 complexes, respectively and therefore, charge migration timescale are predicted to be 550, 550, 500, and 470 attosecond, respectively, for these complexes. This prediction is clearly evident in dynamics calculation presented in Figures 4, 6 and 8. Therefore, the timescale

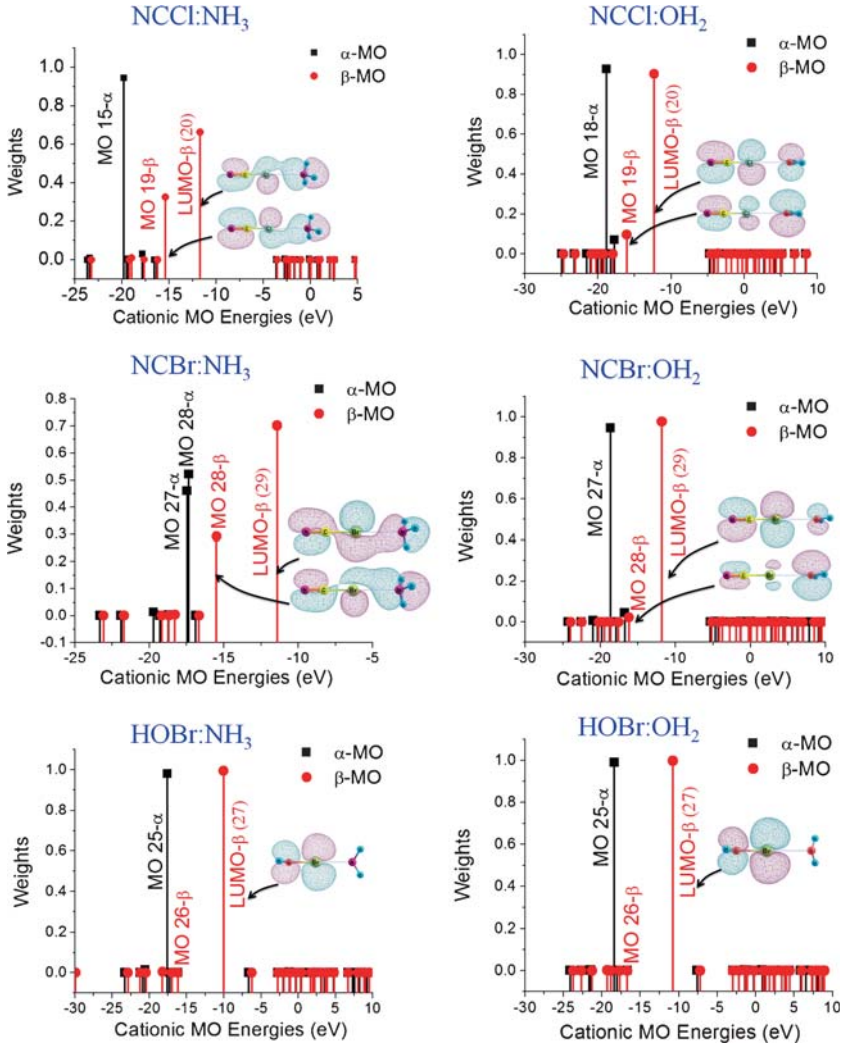

Figure 9. Weight of the neutral HOMO on all stationary cationic MOs of NCCl:NH_3, NCCl:OH_2, NCBr:NH_3, NCBr:OH_2, HOBr:NH_3, and HOBr:OH_2, computed at the wB97XD/6-31+G(d,p) level of theory.

of the attosecond charge migration depends on the energy difference between the LUMO-β and HOMO-β stationary cationic orbitals which together represent the initial hole density in the halogen bonded complex.

On the other hand, the HOMO density is mostly represented by one stationary cationic MO, namely LUMO-β (Figure 9), for both HOBr:NH_3 and HOBr:OH_2 complexes. Therefore, the hole, which is created initially at the neutral HOMO, stays localized on the same site and as a result, no hole migration is observed in these halogen bonded complexes.

Two spin levels appear (denoted as α and β spins) under the unrestricted-self consistent field (unrestricted-SCF) scheme. The time evolution of different spin orbitals depends on the weight of HOMO on these cationic orbitals. The time evolution of the α and β densities are shown in Figure S2 in Supporting Information, taking an illustrative example of NCCl:NH_3 complex. It is clear in the figure that only α-15 cationic MO has the maximum contribution to the neutral HOMO, whereas in case of β orbitals, HOMO is represented as a linear combination of β-19 MO and LUMO-β (β-20) orbitals. Therefore, β-densities contribute maximum to the overall hole density evolution in the attosecond timescale. This is true for all complexes which exhibit charge migration.

3.2b *Strength of Electron Correlation*: Our investigation of charge migration dynamics through halogen bonds is based on one electron molecular orbital picture formalism at the DFT level and that is why we believe that electron-electron relaxation and correlation are the only driving force for this charge migration. In order to visualize the effect of strength of electron correlation on the charge migration dynamics, we have plotted charge migration timescale (which is defined as ($\tau/2$), where the period (τ) for the hole migration is nothing but an oscillation of the charge between these two stationary cationic orbitals) as a function of correlation energy. In the Hartree-Fock approximation, each electron sees the average density of all other electrons and that is why it is considered that HF-method does not include any electron correlation. On the other hand, MP2 and DFT capture good amount of 'correlation energy' at low computational cost. Therefore, difference between MP2- or DFT-binding energy and HF-binding energy can recover a large fraction of the correlation energy for the noncovalent bonds. Figure 10 plots charge migration timescale for different (1:1) complexes containing NH_3 and H_2O molecules as a function of correlation energy, which clearly exhibits a trend: higher the correlation energy, faster the charge migration timescale.

As the present work points to an important role of the correlation interaction in the attosecond charge migration phenomenon through halogen bonds, one of our future aims is to study charge migration dynamics through halogen bonds using highly correlated wave function based methodologies, such as MP4, CCSD(T) and CASPT2.

3.2c *Effect of Donor and Acceptor*: One of our aims in the present study is to explore the effect of donor molecules (H_2O and NH_3) and acceptor atoms (Cl and Br) on attosecond charge migration dynamics through halogen bonds. Among Cl···O and Br···O halogen bonded complexes, which contain H_2O donor molecule, complexes containing ClF, BrF, Cl_2, ClBr, ClCN and BrCN acceptor molecules show charge migration from the ACl- or ABr-end to the H_2O-end through respective halogen bond. When H_2O is replaced by NH_3 donor molecule, only NCCl:NH_3 and NCBr:NH_3 complexes exhibit charge migration. No charge migration is observed in other complexes, such as FCl:NH_3, FBr:NH_3, ClCl:NH_3, ClBr:NH_3,

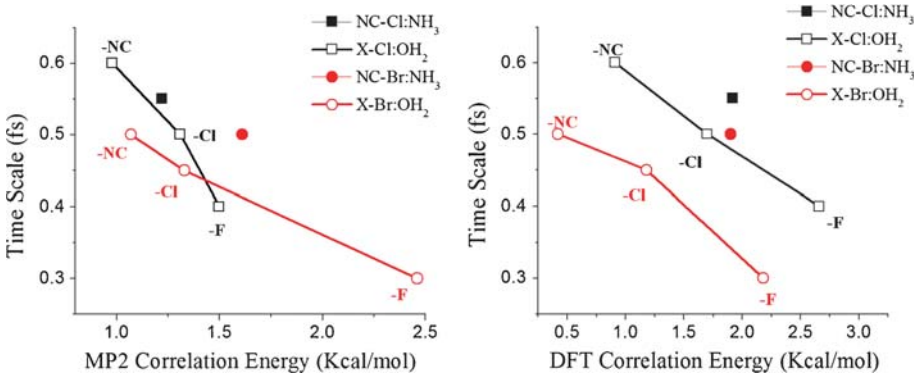

Figure 10. Charge migration time scale is plotted as a function of correlation energy contributed to the halogen bonding interaction for different noncovalent bonded (1:1) complexes.

$HOCl:NH_3$ and $HOBr:NH_3$. For $NCCl:OH_2$ complex charge migrates from the NCCl-end to the H_2O-end, whereas for $NCCl:NH_3$ complex charge migrates from NH_3-end to the NCCl-end. With all these diversities in nature of charge migration as a function of donor and acceptor, a few observations are very systematic and interesting:

(1) FCl and Cl_2 show charge migration when donor molecule is changed from NH_3 to H_2O. This

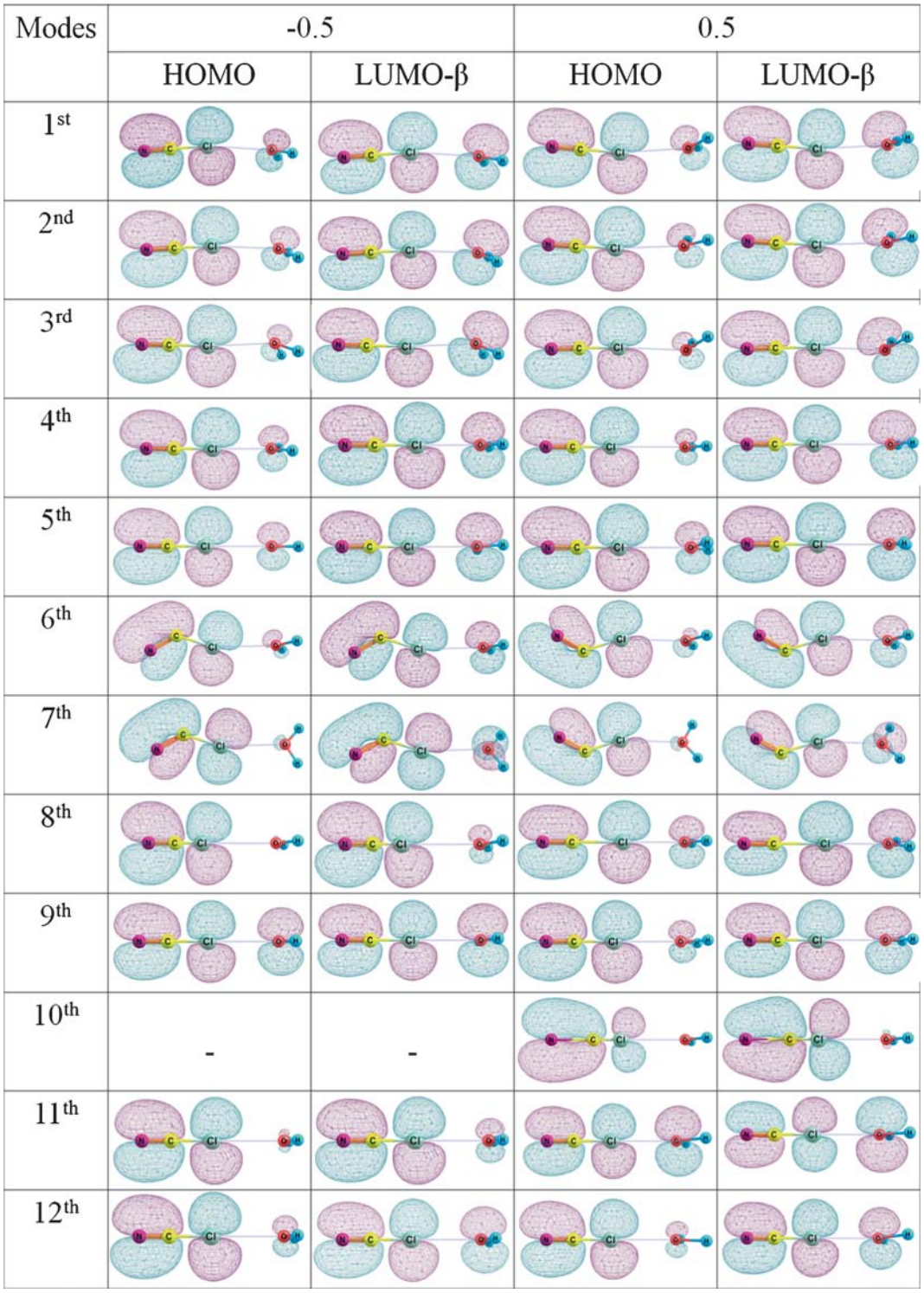

Figure 11. Neutral HOMOs and cationic LUMO-βs at the vertical ion point (VI point) on the D_0 surface for distorted geometries obtained along each normal mode coordinate of $NCCl:OH_2$ complex with new structure coordinate presented as $q_{i,new} = q_{i,opt} \pm 0.5q_{ij}$ (i represents coordinate and j represents vibrational mode). This is computed at the wB97XD/ 6-31+G(d,p) level of theory.

change is also associated with change in halogen bond strength. In general, we find from Figure 2 that binding energy decreases when donor molecule is changed from NH_3 to H_2O. This decrease in binding energy facilitates charge migration through the halogen bond.

(2) The direction of charge migration changes when donor molecule is changed from NH_3 to H_2O. For all complexes containing H_2O, where charge migration occurs, charge migrates from AX-end to H_2O-end. On the other hand, for all complexes containing NH_3 donor molecule, which exhibit charge migration, charge migrates from NH_3-end to AX-end.

(3) Nature of charge migration from complexes containing Br and Cl with single donor molecule (either H_2O or NH_3) does not significantly change. It is only charge migration timescale which is observed to have changed as we replace Br by Cl. It is evident in Figure 10.

3.2d *Effect of Vibration and Rotation*: There are some fundamental difficulties which one faces while studying pure electron-electron correlation- and relaxation-driven hole migration dynamics in isolated molecular clusters.[21] One of the important fundamental problems is that molecules (even in isolated gas phase) do not possess frozen nuclei; they vibrate and rotate (which features the nuclear motion with respect to molecular frame). Molecular vibration and rotation are manifested by change in nuclear configuration. Presence of molecular clusters undergoing vibration and rotation at the experimental temperature is ubiquitous. If the structural change due to vibration influences vertical ionization-induced hole migration, the experimental signal of hole migration can be smeared out due to the presence of vibrationally excited state molecules present in a realistic experimental condition. Therefore, in the present context, it is an important task to investigate the extent to which the molecular vibration influences hole migration triggered by vertical ionization. This task will be able to evaluate significance of our present findings for more realistic experimental conditions.

In order to investigate the effect of vibration on the electron-electron relaxation- and correlation-driven charge migration dynamics through halogen bonds, we have selected NCCl:OH_2 complex as an illustrative example. Analysis of vibrational frequencies at the wB97XD/6-31+G(d,p) level of theory reveals that this complex exhibits total 12 normal modes of vibration. As vertical ionization occurs at the frozen nuclei configuration, we have distorted NCCl:OH_2 complex along the respective normal mode coordinate. In order to see appreciable effect, we have chosen classical turning point geometries obtained along each normal mode coordinate of NCCl:OH_2 complex with new structure coordinate presented as $q_{i,new} = q_{i,opt} \pm 0.5q_{ij}$ (i represents coordinate and j represents vibrational mode). Neutral HOMOs and cationic LUMO-βs at the vertical ion point (VI point) associated with distorted geometries are depicted in Figure 11. Figure 12 compares the extent of charge migration associated with each distorted geometry.

While comparing both Figures 11 and 12, we divide 12 normal modes into 3 categories to elucidate the influence of vibration on attosecond charge migration. 1st category includes 1st, 2nd, 3rd, 4th (+0.50), 5th, 8th (+0.50), 9th (+0.50) and 12th normal modes which have almost no influence of vibration on charge migration dynamics. The HOMOs associated with the distorted geometries along these normal modes are found to be localized at the NCCl-end and corresponding cationic LUMO-βs are found to be delocalized over the complex. Timescale of charge migration remains comparable to that observed for neutral optimized frozen geometry. 2nd category has intermediate effect of vibration on the charge migration dynamics. This category includes 4th (-0.50), 6th, 7th, 9th (−0.50) and 11th (+0.50) modes. On the other hand, the 3rd category features normal modes which significantly affect the charge migration dynamics. This includes only 3 modes, comprising 8th (−0.50), 10th (+0.50) and 11th (−0.50) modes. For these modes HOMO and LUMO-β remain almost the same, indicating cessation of charge migration.

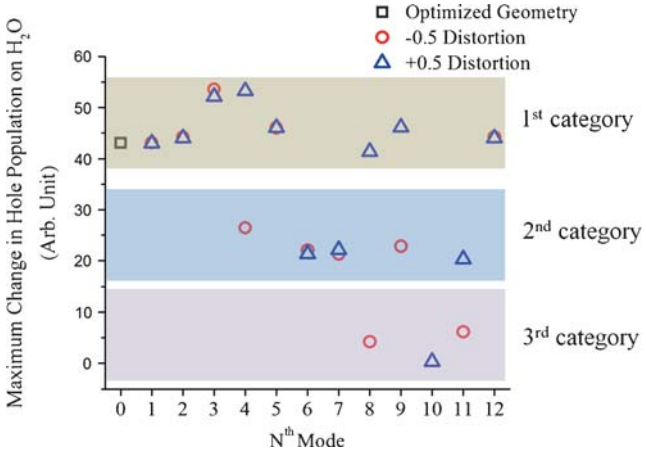

Figure 12. Maximum change in population on the H_2O moiety of NCCl:OH_2 complex for the optimized geometry and for distorted geometries obtained along each normal mode coordinate with displacement, $q_{i,new} = q_{i,opt} \pm 0.5q_{ij}$, computed with the wB97XD DFT functional and the 6-31+G(d,p) basis set.

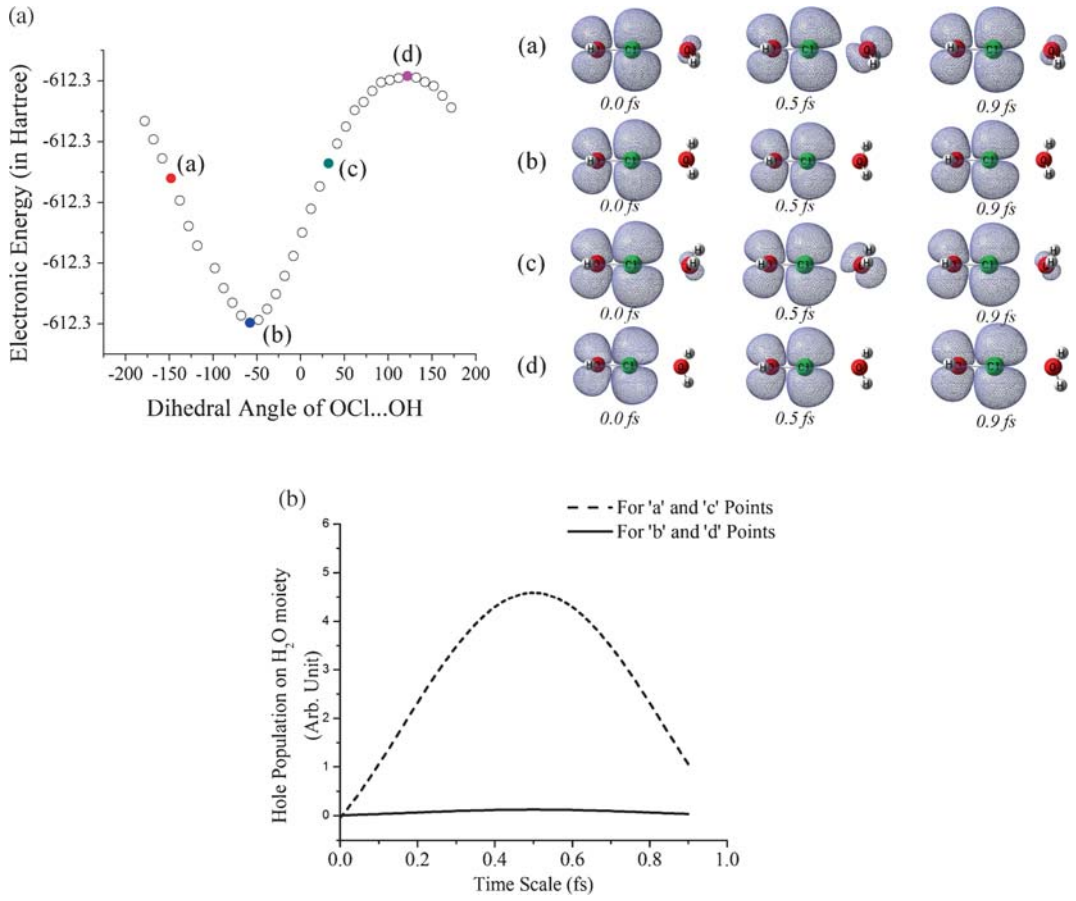

Figure 13. (a) Time evolution of the hole orbital of $HOCl{:}OH_2$ complex for frozen distorted geometries obtained with different dihedral angle of H_2O molecule along the Cl⋯O halogen bond. Computation was performed at the wB97XD/6-31+G(d,p) level of theory. (b) Time evolution of the hole density on the H_2O moiety for the 'a', 'b', 'c' and 'd' configurations.

In the end, we have investigated the effect of rotation on the attosecond charge migration dynamics in halogen bonded complexes. For this purpose, we have considered $HOCl{:}OH_2$ complex as an illustrative example. We have seen that at the neutral equilibrium configuration, this complex does not show charge migration following vertical ionization because both neutral HOMO and cationic LUMO-β densities are identical and both are localized on the ClOH-end of the complex. However, as evident in Figure 13, rotation of H_2O molecule with respect to the Cl⋯O halogen bond may induce charge migration. Two frozen rotational intermediates are shown in Figure 13a ('a' and 'c' configurations), which exhibit non-identical neutral HOMO and cationic LUMO-β, which is suggestive of charge migration at those nuclear configurations. Figure 13b gives a comparison of change of the hole population at the H_2O moiety for four different rotational angles of H_2O moiety along the Cl⋯O bond. Figure 13b infers that relative orientation of the lone pair orbital of donor H_2O can influence hole migration dynamics in Cl⋯O halogen bonded complex.

Undoubtedly, above analysis of effect of rotation and vibration on the attosecond charge migration dynamics through halogen bonds has been performed with little exaggeration of the effect of nuclear motion. Molecular dynamics simulation must be used to decipher the effects in time domain. In fact, currently we are working along that line.

4. Conclusions

The possibility to characterize pure electron-electron relaxation- and correlation-driven charge migration processes and their controlling factors is attracting great interest now-a-days, particularly due to contemporary development of the time-resolved spectroscopic technique using attosecond laser pulses. In the present work, we have elaborately explored the nature of attosecond charge migration dynamics through the Cl⋯N, Br⋯N, Cl⋯O, and Br⋯O halogen bonds using one electron approximation. Furthermore, we have also explored the role of different halogen bond strength, electron

correlation, donor and acceptor, vibration and rotation in attosecond charge migration through halogen bonds.

Present work shows that the door to investigation of the attosecond charge migration through halogen bonds is only beginning to open. So far, only the single electron density scheme has been used to elucidate the attosecond charge migration through halogen bonds. Quite speculative, one can now definitely go beyond single electron density scheme by selecting multi-electronic scheme to describe both escaping electron (defined as Dyson orbital) and the time varying hole density (defined as the difference between the total stationary electron density of the neutral and the time-dependent total density of the initially created cation). Furthermore, in future, one should compare DFT results with time dependent configuration interaction (TDCI) results. We are currently working along that line.

The key theoretical findings of the present work are following:

1. Our present work shows that the timescale of pure electron-electron relaxation and correlation-driven charge migration through the Cl$\cdots$N, Br$\cdots$N, Cl$\cdots$O, and Br$\cdots$O halogen bonds falls in the range of 300–600 attosecond.
2. The primary driving force behind the attosecond charge migration through the Cl$\cdots$N, Br$\cdots$N, Cl$\cdots$O, and Br$\cdots$O halogen bonds is the energy difference (ΔE) between two stationary cationic orbitals (LUMO-β and HOMO-β), which together represent the initial hole density immediately following vertical ionization. This is evident in complexes, such as NCCl:NH_3 NCCl:OH_2, NCBr:NH_3, *etc*. However, if the initial hole density, created immediately after the vertical ionization is represented solely by one stationary cationic MO, namely LUMO-β, hole does not migrate at all. This is evident in complexes such as HOBr:NH_3, HOBr:OH_2, etc.
3. The strength of electron correlation has significant effect on charge migration timescale in Cl$\cdots$N, Br$\cdots$N, Cl$\cdots$O, and Br$\cdots$O halogen bonded clusters. We have found that complexes which show large contribution of electron correlation to the halogen bonding interaction exhibit faster charge migration through the respective halogen bond.
4. Direction of attosecond charge migration is also found to depend on nature of both donor molecules (H_2O and NH_3) and acceptor halogen atoms (Cl and Br). In general, we have found that halogen bonded complexes with H_2O exhibit weaker halogen bonding interaction as compared to those with NH_3 and complexes with water donor show higher tendency of charge migration than those with NH_3.
5. Among different vibrational modes, only a few modes (by distorting the geometry) can actively suppress the attosecond charge migration in halogen bonded clusters.
6. Rotation (by distorting the structure) can induce attosecond charge migration through halogen bond.

Supplementary Information (SI)

Neutral HOMO, cationic LUMO-β and cationic SONO calculated for ACl:NH_3 complexes (where A features F, Cl, OH and CN substituents) are shown in Figure S1. Time evolution of the α and β orbitals in NCCl:NH_3 complex is shown in Figure S2. Supplementary Information is available at www.ias.ac.in/chemsci.

Acknowledgment

This research was supported by the DST-SERB, India (SB/S1/PC-50/2013).

References

1. Metrangolo P and Resnati G 2010 In *Halogen Bonding: Fundamentals and Applications (Structure and Bonding)* (Heidelberg: Springer)
2. Desiraju G R, Ho P S, Kloo L, Legon A C, Marquardt R, Metrangolo P, Politzer P A, Resnati G and Rissanen K 2013 *Pure Appl. Chem.* **85** 1711
3. (a) Jeffrey G A1997 In *An Introduction to Hydrogen Bonding* (New York: Oxford University Press); (b) Scheiner S 1997 In *Hydrogen Bonding: A Theoretical Perspective* (New York: Oxford University Press); (c) Grabowski S J 2006 In *Hydrogen Bonding – New Insights, in Challenges and Advances in Computational Chemistry and Physics* J Leszczynski (Ed.) (Dordrecht: Springer) Vol. 3
4. (a) Metrangolo P and Resnati G 2001 *Chem.–Eur. J.* **7** 2511; (b) Cavallo G, Metrangolo P, Pilati T, Resnati G, Sansoteraand M and Terraneo G 2010 *Chem. Soc. Rev.* **39** 3772; (c) Riley K E and Hobza P 2008 *J. Chem. Theory Comput.* **4** 232; (d) Alkorta I, Blanco F, Solimannejad M and Elguero J 2008 *J. Phys. Chem. A* **112** 10856; (e) Metrangolo P and Resnati G (Eds.) 2008 In *Halogen Bonding: Fundamentals and Applications* (Springer: Berlin) Vol. 126 p.1; (f) Hauchecorne D, Szostak R, Herrebout W A and Veken B J v d 2009 *Chem. Phys. Chem.* **10** 2105; (g) Sarwar M G, Dragisic B, Salsberg L J, Gouliaras C and Taylor M S 2010 *J. Am. Chem. Soc.* **132** 1646; (h) Zierkiewicz W, Michalska D and Zeegers-Huyskens T 2010 *Phys. Chem. Chem. Phys.* **12** 13681; (i) Politzer P, Murray J S and Clark T 2010 *Phys. Chem. Chem. Phys.* **12** 7748; (j) Parisini E, Metrangolo P, Pilati T, Resnati G and Terraneo G 2011

Chem. Soc. Rev. **40** 2267; (k) Stephens S L, Walker N R and Legon A C 2011 *Phys. Chem. Chem. Phys.* **13** 20736; (l) Grabowski S J 2012 *J. Phys. Chem. A* **116** 1838; (m) Erdelyi M 2012 *Chem. Soc. Rev.* **41** 3547; (n) Legon A C 2010 *Phys. Chem. Chem. Phys.* **12** 7736; (o) Piland G B and Jasien P G 2012 *Comput. Theor. Chem.* **988** 19

5. Beratan D N, Onuchic J N, Winkler J R and Gray H B 1992 *Science* **258** 1714
6. deRege P J, Williams S A and Therien M J 1995 *Science* **269** 1409
7. Lin J, Balabin I A and Beratan D N 2005 *Science* **310** 1311
8. Chang S, He J, Kibel A, Lee M, Sankey O, Zhang P and Lindsay S 2009 *Nat. Nanotechnol.* **4** 297
9. Kurlancheek W and Cave R J 2006 *J. Phys. Chem. A* **110** 14018
10. (a) Bolton O, Lee K, Kim H-J, Lin K Y and Jim J 2011 *Nature Chem.* **3** 205; (b) Priimagi A, Cavallo G, Metrngolo P and Pesnati G 2013 *Acc. Chem. Res.* **46** 2686; (c) Nguyen H L, Horton P N, Hursthouse M B, Legon A C and Bruce D W 2004 *J. Am. Chem. Soc.* **126** 16
11. (a) Bhattacharya A and Bernstein E R 2011 *J. Phys. Chem. A* **115** 10679; (b) Bhattacharya A, Shin J-W, Clawson K and Bernstein E R 2010 *Phys. Chem. Chem. Phys.* **12** 9700
12. (a) Lünnemann S, Kuleff A I and Cederbaum L S 2008 *J. Chem. Phys.* **129** 104305; (b) Cederbaum L S and Zobeley J 1999 *Chem. Phys. Lett.* **307** 205; (c) Kuleff A I, Breidbach J and Cederbaum L S 2005 *J. Chem. Phys.* **123** 044111
13. (a) Remacle F and Levine R D 2006 *Proc. Natl. Acad. Sci. U.S.A.* **103** 6793; (b) Remacle F and Levine R D 2007 *Z. Phys. Chem.* **221** 647; (c) Remacle F and Levine R D 2006 *J. Chem. Phys.* **125** 133321; (d) Periyasamy G, Levine R D and Remacle F 2009 *Chem. Phys.* **366** 129
14. Chandra S, Periyasamy G and Bhattacharya A 2015 *J. Chem. Phys.* **142** 244309
15. Chandra S, Rana B, Periyasamy G and Bhattacharya A 2016 *Chem. Phys.* **472** 61
16. Marcus R A and Sutin N 1985 *Biochim. Biophys. Acta* **811** 265
17. (a) Kuleff A I and Cederbaum L S 2014 *J. Phys. B: At. Mol. Opt. Phys.* **47** 124002; (b) Kus T, Mignolet B, Levine R D and Remacle F 2013 *J. Phys. Chem. A* **117** 10513
18. (a) Yanai T, Tew D and Handy N 2004 *Chem. Phys. Lett.* **393** 51; (b) Chai J-D and Head-Gordon M 2008 *Phys. Chem. Chem. Phys.* **10** 6615
19. Frisch M J, Trucks G W, Schlegel H B, Scuseria G E, Robb M A, Cheeseman J R, Scalmani G, Barone V, Mennucci B, Petersson G A, Nakatsuji H, Caricato M, Li X, Hratchian H P, IzmaylovA F, Bloino J, Zheng G, Sonnenberg J L, Hada M, Ehara M, Toyota K, Fukuda R, Hasegawa J, Ishida M, Nakajima T, Honda Y, Kitao O, Nakai H, Vreven T, Montgomery J A Jr, Peralta J E, Ogliaro F, Bearpark M, Heyd JJ, Brothers E, Kudin K N, Staroverov V N, Kobayashi R, Normand J, Raghavachari K, e Rendell A, Burant J C, Iyengar S S, Tomasi J, Cossi M, Rega N, Millam N J, Klene M, Knox J E, Cross J B, Bakken V, Adamo C, Jaramillo J, Gomperts R, Stratmann R E, Yazyev O, Austin A J, Cammi R, Pomelli C, Ochterski J W, Martin R L Morokuma K, Zakrzewski V G, Voth G A, Salvador P, Dannenberg J J, Dapprich S, Daniels A D, Farkas Ö, Foresman J B, Ortiz J V, Cioslowski J and Fox D 2009 *J. A. Gaussian 09, Revision* D.01, Inc, Wallingford CT
20. Boys S F and Bernardi F 1970 *Mol. Phys.* **19** 553
21. Leone S R, McCurdy C W, Burgdorfer J, Cederbaum L, Chang Z, Dudovich M, Feist J, Greene C, Ivanov M, Kienberger R, Keller U, Kling M, Loh Z-H, Pfeiffer T, Pfeiffer A N, Santra R, Schafer K, Stolow A, Thumm W and Vrakking M 2014 *Nat. Photon.* **8** 162